

# UC San Diego

## UC San Diego Previously Published Works

### Title

Transmembrane domain helix packing stabilizes integrin  $\alpha$ IIb  $\beta$ 3 in the low affinity state

### Permalink

<https://escholarship.org/uc/item/6nr610jd>

### Journal

Journal of Biological Chemistry, 280(8)

### ISSN

0021-9258

### Authors

Partridge, Anthony W  
Liu, Shouchun  
Kim, Sanguk  
et al.

### Publication Date

2005-02-01

Peer reviewed

**Transmembrane Domain Helix Packing Stabilizes Integrin  $\alpha$ IIb $\beta$ 3 in the Low  
Affinity State**

Anthony W. Partridge<sup>1,5</sup>, Shouchun Liu<sup>2,5</sup>, Sanguk Kim<sup>3</sup>, James U. Bowie<sup>3</sup>, Mark H.  
Ginsberg<sup>1,4</sup>

<sup>1</sup>The Department of Medicine, University of California San Diego

<sup>2</sup>Nuvelo Inc., South San Francisco, CA

<sup>3</sup>Department of Chemistry and Biochemistry, University of California Los Angeles

<sup>4</sup>To whom correspondence should be addressed at: 9500 Gilman Drive, Leichtag 181,  
Mail code 0726, La Jolla CA 92093-0726.

**Email:** [mhginsberg@ucsd.edu](mailto:mhginsberg@ucsd.edu)

**Telephone:** 858-822-6432

**Fax:** 858-822-6458

<sup>5</sup>These two authors contributed equally to this work.

Running Title: Integrin activation and transmembrane domain packing

Key Words: Signal Transduction, Integrin, Transmembrane domain, membrane protein,  
structure

## SUMMARY

Regulated changes in the affinity of integrin adhesion receptors (“activation”) play an important role in numerous biological functions including hemostasis, the immune response, and cell migration. Physiological integrin activation is the result of conformational changes in the extracellular domain initiated by the binding of cytoplasmic proteins to integrin cytoplasmic domains. The conformational changes in the extracellular domain are likely caused by disruption of intersubunit interactions between the  $\alpha$  and  $\beta$  transmembrane (TM) and cytoplasmic domains. Here, we reasoned that mutation of residues contributing to  $\alpha/\beta$  interactions that stabilize the low affinity state should lead to integrin activation. Thus, we subjected the entire intracellular domain of the  $\beta_3$  integrin subunit to unbiased random mutagenesis and selected for activated mutants. Twenty five unique activating mutations were identified in the TM and membrane-proximal cytoplasmic domain. In contrast, no activating mutations were identified in the more distal cytoplasmic tail, suggesting that this region is dispensable for the maintenance of the inactive state. Among the 13 novel TM domain mutations that lead to integrin activation were several informative point mutations that, in combination with computational modeling, suggested the existence of a specific TM helix-helix packing interface that maintains the low affinity state. The interactions predicted by the model were used to identify additional activating mutations in both the  $\alpha$  and  $\beta$  TM domains. We therefore propose that helical packing of the  $\alpha$  and  $\beta$  TM domains forms a clasp that regulates integrin activation.

## INTRODUCTION

Integrin heterodimers are essential for the development and functioning of multicellular animals as they mediate cell migration, cell adhesion, and can influence gene expression and cell proliferation(1). All integrin heterodimers are composed of single pass Type I transmembrane (TM) protein subunits,  $\alpha$  and  $\beta$ . A central feature of these receptors is their capacity for rapid changes in their adhesive function mediated by changes in their ligand binding affinity, operationally defined here as “activation.” The prototypical integrin, platelet  $\alpha$ IIb $\beta$ 3, is activated through interactions of the cytoplasmic integrin tails (~ 20 and 47 residues for alpha and beta tails, respectively) with intracellular proteins, such as talin (2). These interactions initiate a long-range conformational change in the large extracellular domains (> 700 residues each) resulting in high affinity binding of fibrinogen, von Willebrand factor, and fibronectin and consequently platelet aggregation and adherence to the vessel wall (1).

Initial mutational studies suggested that a salt bridge between  $\alpha$ IIbArg<sup>995</sup> and  $\beta$ 3Asp<sup>723</sup> helps maintain the integrin in the low affinity state by forming part of an interactive face between  $\alpha$  and  $\beta$  subunit cytoplasmic domains (3). Protein engineering studies from Springer’s lab have further advanced the idea that specific integrin  $\alpha/\beta$  interactions maintain the low affinity conformation of the receptor. In particular, enforced association of either the C terminal regions of the extracellular domains (4) or of the cytoplasmic domains (5) leads to expression of an inactive integrin. Furthermore, during physiological integrin activation, changes in fluorescence resonance energy transfer between fluorophores joined to the  $\alpha$ L and  $\beta$ 2 cytoplasmic domains are

consistent with cytoplasmic domain separation(6). Finally, constraining the integrin  $\alpha$  and  $\beta$  transmembrane domains with inter-subunit disulfide bonds blocks integrin activation from inside the cell. However, this constraint does not prevent activation by divalent cations and antibodies that activate by binding to the extracellular domain(7). Taken together, these data suggest that default low affinity state of integrins is maintained by interactions between integrin  $\alpha$  and  $\beta$  subunits and that physiological activation occurs when cytoplasmic domain ligands, such as talin, disrupt these interactions.

Support for the idea that an Arg<sup>-995</sup>-Asp<sup>723</sup> salt bridge is an important constraint for the low affinity state comes from a nuclear magnetic resonance (NMR) spectroscopy study (8). Specifically, in isolated  $\alpha$ IIb and  $\beta$ 3 cytoplasmic domain peptides the salt-bridge was identified as part of a helical interface between the membrane-proximal regions of  $\alpha$  and  $\beta$  subunits. Furthermore, this interaction was disrupted by talin, supporting the notion that disruption of this salt-bridge is involved in integrin activation(8). However, other groups have failed to observe intersubunit interactions in the membrane-proximal region suggesting that it is of relatively low affinity(9;10). Therefore, additional intracellular regions of the receptor could contribute  $\alpha/\beta$  interactions to “clasp” it into the low affinity state. Indeed, *in vitro* model systems identified heterodimeric interactions between integrin  $\alpha$  and  $\beta$  transmembrane (TM) domains(11) and such interactions have also been suggested by molecular modeling(12;13) and disulfide cross-linking approaches(7). Mutation of residues contributing to  $\alpha/\beta$  interactions that stabilize the low affinity state should lead to integrin activation. Thus, we subjected the entire intracellular domain (cytoplasmic plus TM domain, Fig. 1) of the  $\beta$ 3 integrin subunit to unbiased random mutagenesis and selected

for activated mutants. Through this analysis, we have confirmed the importance of the membrane-proximal domain in maintenance of the low affinity state. In contrast, no activating mutations were identified in the more distal cytoplasmic tail suggesting that this region is dispensable for the maintenance of the inactive state. This approach also identified 13 novel TM domain mutations that lead to integrin activation. Amongst these were several informative point mutations that suggested the existence of a TM helix packing interface that maintains the low affinity state. Computational modeling indicates that these mutations disrupted intersubunit interactions either directly or indirectly by altering helical length/tilt angle. The interactions predicted in the model were used to create additional activating mutations in both the  $\alpha$  and  $\beta$  TM domains. We therefore propose that  $\alpha$  and  $\beta$  TM regions interact to form a clasp that constrains integrin activation.

## EXPERIMENTAL PROCEDURES

### Cell Culture, Cell Lines, and Reagents

Chinese hamster ovary (CHO) cells were obtained from American Type Culture Collection (ATCC) and cultured in Dulbecco's modified Eagle's medium with 10% fetal bovine serum (FBS), 1% non-essential amino acids (Sigma), 50 units of penicillin/ml, and 50  $\mu$ g of streptomycin sulfate/ml in a 37°C tissue culture incubator.  $\alpha$ IIBc5 cells, an  $\alpha$ IIB integrin subunit-expressing CHO cell line, were created by transfecting CHO cells with CDM8 vectors encoding the  $\alpha$ IIB integrin subunit along with CD Neo plasmid. Stable colonies were selected with neomycin for two weeks. The pooled stable colonies were subsequently infected with an adenovirus encoding  $\beta$ 3 integrin subunit, and sorted for single cells expressing  $\alpha$ IIB $\beta$ 3 integrin. Each individual stable clone was then examined for the absence of  $\beta$ 3 subunit to make sure that the adenovirus had not integrated into the genome. The clones that do not express  $\beta$ 3 subunit were then transiently transfected with a plasmid that encodes  $\beta$ 3 and tested for expression of  $\alpha$ IIB $\beta$ 3. The clones that revealed normal expression of  $\alpha$ IIB $\beta$ 3 after transient expression of  $\beta$ 3 subunit were then used for further studies. The anti- $\alpha$ IIB $\beta$ 3 antibodies D57, PAC1, and Anti-LIBS6, as well as Ro43-5054, an  $\alpha$ IIB $\beta$ 3-specific peptide-mimetic competitive inhibitor, have been described (14-17). The D57 antibody was biotinylated with biotin-N-hydroxy-succinimide (Sigma) (B-D57) according to manufacturer's instructions.

## Construction of Random Mutagenic cDNA Libraries of $\beta 3$ Integrin Subunit

To facilitate construction of random mutagenic cDNA libraries of transmembrane and cytoplasmic domains of  $\beta 3$  integrin subunit, an *Sph* I restriction enzyme site was created via a silent mutation at nucleotide 1899 (C->A) of  $\beta 3$  cDNA sequence using site-directed mutagenesis. The *Sph* I site-containing full-length  $\beta 3$  cDNA was then subcloned into a hygromycin-resistant derivative of CDM8 expression vector (Invitrogen), CDHYG, to create a wide-type  $\beta 3$ -expressing vector, CDHYG3A.*Sph* I. Transiently transfection of this construct in an  $\alpha$ IIB-expressing Chinese hamster ovary (CHO) cell line,  $\alpha$ IIBC5, or co-transfection with wild-type  $\alpha$ IIB cDNA in CHO cells, resulted in a protein product with identical properties to that of wild-type  $\alpha$ IIB $\beta 3$ . Specifically, the mutant species was immunoprecipitated by D-57 (not shown), an antibody against the extracellular domains of  $\alpha$ IIB $\beta 3$  and was found to be in the low affinity state because it failed to bind PAC1, a monoclonal antibody specific for the high affinity state of  $\alpha$ IIB $\beta 3$ . Furthermore, the *Sph* I construct gained PAC1-binding ability with treatment of an  $\alpha$ IIB $\beta 3$ -activating antibody, Anti-LIBS6 but failed to bind PAC1 in the presence of Ro43-5054, an  $\alpha$ IIB $\beta 3$ -specific peptide-mimetic competitive inhibitor (not shown). Thus, this silent mutation does not interfere with the normal expression or function of  $\beta 3$  integrin subunit. The spiked mega primer method was chosen to generate random mutagenic cDNA libraries of  $\beta 3$  cytoplasmic and transmembrane domains (18). Specifically, the  $\beta 3$  transmembrane and cytoplasmic domains were divided into four “windows” of 66 nucleotides each with a nine nucleotides overlap between windows (Fig. 1). Spiked oligonucleotide primers corresponding to each window (Fig. 1) were synthesized with a contamination level of

1.5% of incorrect phosphoramidites, i.e., 0.5% of each of the three other bases.

Polymerase chain reaction (PCR) was performed using the spiked primer (S.M.P., Fig. 2A) for each window and a 3' reverse primer that contains an *Xba* I restriction enzyme site (R.P., Fig. 2A). For second round of PCR reaction (PCR-II, Fig. 2A), the PCR-I product (megaprimer) was used as a reverse primer. PCR reaction was performed with the megaprimer and a forward primer that contains the *Sph* I site (F.P., Fig. 2A). Products from PCR-II were then subcloned into *Sph* I-*Xba* I sites of CDHYG3A.*Sph* I. The efficiency of random mutagenesis was assessed by cDNA sequencing of 10 randomly-picked transformants from each window. cDNA sequencing indicated that about 70% of inserts in each window contained 1, 2, or 3 point mutations, which is in the reasonable range of efficiency for random mutagenesis. Theoretically, for a window of 66 nucleotides, 150,000 transformants should cover 99% of the possible one-base changes and ~75% of the possible two-base changes. Therefore, a random mutagenic cDNA library containing ~200,000 transformants for each window of transmembrane and cytoplasmic domains of  $\beta$ 3 subunit was constructed by large-scale preparation of transformants, and used for subsequent transfection into  $\alpha$ IIbC5 cells and identification of activating mutations in the  $\beta$ 3 subunit.

### **Site Directed Mutagenesis**

Site-directed mutations in both the  $\alpha$ IIb and  $\beta$ 3 subunits were generated using the QuikChange mutagenesis kit (Stratagene) and pCDM8 vectors containing the integrin subunits. Mutants were confirmed by DNA sequencing.

## Flow Cytometry

Random mutagenic cDNA library corresponding to each window of  $\beta 3$  transmembrane and cytoplasmic domains was transfected into  $\alpha$ IIC5 cells by electroporation. Stable colonies were selected for 2 weeks in the presence of both hygromycin (750  $\mu$ g/ml) and neomycin (750  $\mu$ g/ml). About  $5 \times 10^6$  cells from pooled stable colonies from each window were then individually sorted on a FACStar Plus (Becton Dickinson) using two-color flow cytometry. The biotinylated monoclonal antibody, B-D57 was used to detect expression of  $\alpha$ IIB $\beta$ 3, while PAC1, an activation specific, monoclonal IgM antibody was used to assess activation state of the  $\alpha$ IIB $\beta$ 3 integrin. For single cell sorting, the pooled stable colonies from each window ( $\sim 5 \times 10^6$  cells/each window) were resuspended by treatment with trypsin and double-stained as described (19;20). Rare cells that exhibited both bright phycoerythrin staining (D57) and fluorescein isothiocyanate (FITC) staining (PAC1) were individually sorted into 96-well plates.

FACS analysis of isolated clonal cell lines was performed on a FACScan using both B-D57 and PAC1 antibodies as described (19;20). PAC1 staining in the presence of Ro43-5054 (2  $\mu$ M) was used to estimate non-specific binding. In some cases, treatment with Anti-LIBS6 was used to estimate maximal PAC1 binding, since Anti-LIBS directly induces  $\alpha$ IIB $\beta$ 3 binding to PAC1 regardless of the status of cellular activation mechanism (15).

For re-transfection analysis,  $\alpha$ IIBc5 cells were transfected with plasmid CDHYG3A. *Sph* I which encodes wild-type  $\beta 3$  or  $\beta 3$  that contains each identified mutation, using Lipofectamine (Life Technologies) following the manufacturer's instructions. Forty-eight hours after transfection, the transfected cells were stained with B-D57 and PAC1 in the

presence and absence of Ro43-5054, and FACS analysis was performed as described above.

Cytometric analysis of the site directed mutations was done by co-transfection of the pCDM8 plasmids containing the  $\alpha$ IIb and  $\beta$ 3 subunits with Plus reagent and lipofectamine. (Life Technologies). Forty-eight hours after transfection, the transfected cells were stained with B-D57 and PAC1 in the presence and absence of Ro43-5054 and AntiLIBS6, and FACS analysis was performed as described above. Activation index was calculated by using the formula  $(F-F_0)/(F_{max}-F_0)$ , where  $F$ =PAC1 binding,  $F_0$ = PAC1 binding in the presence of Ro43-5054, and  $F_{max}$ =PAC1 binding in the presence of antiLIBS 6.

### **Reverse Transcriptase-PCR, Subcloning, and Sequencing of $\beta$ 3 Integrin Subunit**

Total cellular RNA from each individual cell line was isolated using TRIzol (GIBCO/BRL). cDNA was synthesized using oligo-dT primer and the cDNA Cycle kit (Invitrogen), and PCR was performed following the manufacturer's instructions. PCR products were digested with restriction enzymes *Sph* I and *Xba* I to create a fragment of ~ 550 bp. This *Sph* I-*Xba* I fragment was then subcloned into the *Sph* I-*Xba* I sites of CDHYG3A. *Sph* I vector and sequenced using primers derived from CDHYG3A. *Sph* I plasmid but outside of the *Sph* I-*Xba* I region. To eliminate possible PCR errors, at least four clones were sequenced for each mutant cell line.

## Computer Simulations

The modeling procedures for TM helix oligomerization were described elsewhere (21). Briefly, the TMD sequences of integrin  $\alpha$ IIb and  $\beta$ 3 subunits were built into uniform  $\alpha$ -helices having the backbone torsion angles of  $\phi = -65^\circ$  and  $\psi = -40^\circ$ . Their TMD sequences of  $\alpha$ IIb and  $\beta$ 3 were aligned based on the glycosyl mapping data (22;23). Side chain rotamers were chosen using the backbone-dependent rotamer library program SCWRL (24). Four hundred potential helix packings were first generated using a Monte Carlo search procedure as described (21). The  $\alpha$ IIb and  $\beta$ 3 TMD dimeric structures were then filtered to remove the structures incompatible with the bilayer constraints. Then, we clustered the remaining structures by C $\alpha$  RMS distances using NMRCLUSTER(25), which resulted two equally populated clusters: one with crossing point near the N-terminus and the other with a crossing point close to C-terminus. Both models were evaluated for consistency with the experimental results (see below).

## RESULTS AND DISCUSSION

### **Random Mutagenesis Identifies Novel Integrin Activating Mutations in the TM and Membrane-Proximal Cytoplasmic Regions of $\beta 3$**

To generate the  $\beta 3$  random mutants, we used CDHYG3A.*Sph* I as a template and spiked oligonucleotide primers corresponding to four overlapping windows that cover the entire  $\beta 3$  intracellular domain (Fig. 1). Using the protocol outlined (see Methods and Fig. 2) a cDNA library containing ~200,000 transformants for each window was constructed by large-scale preparation of transformants, and used for subsequent transfection into an  $\alpha$ IIB expressing cell line ( $\alpha$ IIB C5 cells) and identification of activating mutations in the  $\beta 3$  subunit. We developed a library of stable cell lines and selected activated  $\alpha$ IIB $\beta 3$  integrin mutants, by their binding to PAC1, an antibody specific for activated  $\alpha$ IIB $\beta 3$ (15) (Fig. 3A, R2). Using this approach we isolated 91 and 192 cell lines bearing activated  $\alpha$ IIB $\beta 3$  from window I and II, respectively (Table I). In contrast, only 5 cell lines were isolated from either window III or window IV (Table I). Thus, mutations in the membrane-distal segments of the  $\beta 3$  cytoplasmic domain encoded by regions III and IV were less likely to activate  $\alpha$ IIB $\beta 3$  integrin.

The cell lines expressing activated integrin  $\alpha$ IIB $\beta 3$  could have arisen as a consequence of mutations within the target window, from adventitious mutations elsewhere in the integrin, or from mutations in genes that indirectly control integrin activation. To identify mutations in the target window that activated  $\alpha$ IIB $\beta 3$ , we sequenced cDNA clones obtained from  $\beta 3$  reverse transcriptase-PCR (RT-PCR) amplicons spanning this region. To confirm that sequenced mutations were responsible

for integrin activation, these amplicons were used to replace this region in wild type  $\beta 3$ , the resulting plasmids were transfected into  $\alpha \text{IIb} \beta 3$  cells and tested for PAC1 binding in the presence and absence of Ro43-5054. When the transiently expressed mutant integrin was able to bind PAC1, and this PAC1 binding was inhibited by Ro43-5054, we concluded that the mutation was responsible for the activation of  $\alpha \text{IIb} \beta 3$ . A total of 25 unique mutations in the transmembrane and membrane-proximal region of cytoplasmic domain of  $\beta 3$  subunit were thus identified, and there were multiple examples of the same mutations present in different clonal cell lines (Fig. 4). Thirteen of them were found amino terminal of Lys<sup>716</sup> in the presumptive transmembrane domain and twelve were in the membrane-proximal region of cytoplasmic domain (Fig. 5). No mutation was identified that only affected the region of the cytoplasmic domain C-terminal of Asp<sup>723</sup> (Fig 5). The absence of activating mutations C terminal of Asp<sup>723</sup> indicates that the C terminus of  $\beta 3$  is not involved in maintenance of the low affinity state of the integrin. The presence of such mutations in the membrane-proximal and transmembrane domains suggests that these sites are important in regulating integrin activation.

### **Activating mutations are predicted to alter the TM helix length**

We had previously established the importance of the membrane-proximal domains of the  $\alpha$  and  $\beta$  subunits in regulating integrin activation (20). In consequence, we focused our attention on the numerous mutations in the transmembrane domain. Many of these mutations would be predicted to shorten the  $\beta$ -subunit TM helix (i.e. fewer residues embedded in the membrane) by deletion of one or more residues or by introduction of a charged residue (Table II). Indeed, the majority of the mutations (9/13) would be

expected to disrupt or shorten the TM helix. Previous glycosylation-mapping studies(22;23) indicated that activating mutations in the membrane-proximal domain can shorten the TM helix. The present results extend those findings by showing that such mutations throughout the TM helix activate the integrin.

### **Mutagenesis of predicted TM packing residues activates $\alpha$ IIb $\beta$ 3**

A subset (4/13) of the membrane-embedded activating mutations had no obvious effect on TM helical length. This suggests that the TM segments help stabilize the inactive state through sequence-specific interactions. To investigate this possibility, we used a Monte Carlo simulation method(21) to produce a first approximation of the intersubunit packing of integrin TM domains. We caution that this method assumes idealized rigid  $\alpha$  helices and disregards potential changes in membrane insertion. However, several reports indicate that this protocol does yield models that conform well to known the structural and functional data(26-29). Here, the resulting output predicted two alternative structures, one with the TM helices packing near the C-termini (Structure A) and another with the helices packing close to the N-termini (Structure B) (Fig. 6).

The random mutagenesis data focused our attention on Structure A since all of the uncharged activating point mutations clustered in the C-terminal region of the  $\beta$ 3 TM domain (G708S, A711T+T720A, I714T) (Fig. 5). Indeed, each of these mutations affected a residue predicted to be a helical contact in Structure A (Fig. 6B). Three additional site directed mutants were employed to test the hypothesis that the interhelical interface predicted in Structure A functioned as a clasp to maintain the integrin in the low affinity state (*vide infra*).

The  $\beta 3(G708S)$  mutation was strongly activating. Previous studies (30) showed that introduction of an Asn at this position activated  $\alpha IIb\beta 3$  and suggested that it did so by forming hydrogen bonds that favor  $\beta 3$  homoligomerization. The Ser substitution could also, in principle, lead to enhanced  $\beta 3$ - $\beta 3$  interactions through such a mechanism. However, the weakly polar nature of the Ser side chain coupled with the observation that insertion of the bulky aliphatic Ile residue at this position ( $\beta 3(G708I)$  mutation) was strongly activating suggest that a Gly residue is strictly required at this position for efficient  $\alpha/\beta$  TM packing. (Fig. 7A, B, C).

The packing motif in Structure A allowed us to identify an additional Van der Waals packing residue that helps stabilize the inactive state since the apolar to apolar I704A mutation resulted in an activated integrin (Fig. 7B, C). As well, the Structure A model predicted that  $\alpha IIb$  TM residues would pack against the identified  $\beta 3$  residues. Accordingly, we substituted a bulky Ile residue for  $\alpha IIb$  Thr<sup>981</sup>, the residue predicted to pack against  $\beta 3$  Gly<sup>708</sup> (Fig. 6B). The observation that this mutant activated  $\alpha IIb\beta 3$  supports the packing of Thr<sup>981</sup> against Gly<sup>708</sup> – an interaction that would be stabilized by both Van der Waals packing and a potential C $\alpha$ /hydroxyl hydrogen bond. Overall, both random mutagenesis and site-directed mutagenesis (Fig. 7C) support the hypothesis that the specific packing of the C-terminal portions of  $\alpha IIb$  and  $\beta 3$  transmembrane helices against each other maintains the low affinity state of integrin  $\alpha IIb\beta 3$ .

Activation by mutagenically dissociating the integrin TM helices is consistent with reports that suggest that activation is associated with separation of the cytoplasmic domains(2;6). However, the unbiased random mutagenesis approach identified a preponderance of activating TM domain mutations predicted to shorten the  $\beta 3$  TM

domain indicating that TM helix shortening can also lead to integrin activation. In agreement with this mechanism, previous glycosylation mapping studies suggested that the membrane-proximal domains of the  $\alpha$  and  $\beta$  subunits can reside with the membrane bilayers and that certain activating mutations in this region(22;23) result in a shortened TM domain.

How might shortening the TM domain lead to disruption of intracellular  $\alpha/\beta$  interactions and consequent integrin activation? In order to avoid hydrophobic mismatch with the fixed width of the membrane bilayer, a shortened TM helix would change its membrane tilt angle and associated register with neighboring helices (31). Since helix-helix packing is dependent on specific crossing angles and specific in-register side chain arrays, changes to TM helical length would break the proposed clasp. Previous observations showing that  $\alpha$ IIb sequences with a shortened TM segment (7) lost the ability to induce a periodic disulfide crosslinking pattern of the  $\alpha$ IIb and  $\beta$ 3 transmembrane helices support this notion. In addition, the inactive state intersubunit interactions at membrane-proximal level could cooperate with the TM packing to help maintain the  $\alpha/\beta$  association. Importantly, talin has been shown to bind to the membrane-proximal region(8;32;33)– an event that appears to be important for  $\alpha$ IIb $\beta$ 3 activation(33). This interaction could contribute to the physiological activation of integrins in two separate but related ways. First, one consequence of talin binding to this region would be to displace the membrane-proximal domain from the bilayer, thereby shortening the TM domain. As noted above this process would likely lead to separation of the intracellular domains. Talin binding could also directly disrupt the cooperative

membrane proximal/TM clasp by breaking the Arg<sup>995</sup>-Asp<sup>723</sup> salt bridge(8) and associated intersubunit interactions.

Our findings also have implications for integrin-mediated biochemical signals that control cell shape, cell migration, proliferation, and survival. The capacity of integrins to deliver such signals depends on their occupancy with resultant conformational change in the integrin(34) in combination with receptor clustering(35;36). These conformational changes are associated with a dramatic change in the quaternary structure of the integrin, resulting in a switch from a “bent” conformation observed in the crystal structure(37) to an extended one(38) that features a C-terminal separation(39) that would disrupt the TM helical packing proposed here. This disruption could lead to the changes in the intracellular interactions of occupied integrins manifested by focal adhesion targeting and trans-dominant inhibition(34;40). Furthermore, the work of Li et al shows that isolated integrin  $\alpha$  and  $\beta$  TM peptides homoligomerize(10)– a process that could contribute to integrin clustering. This suggests a sequential model in which  $\alpha/\beta$  transmembrane separation might then be followed by homoligomerization to favor receptor clustering(10;41). Strikingly, Li et. al.’s mutational studies identify  $\beta 3$  Gly<sup>708</sup> as an important packing residue for  $\beta 3$  homoligomerization and suggest that homoligomerization may occur after TM separation(30). Our findings indicating that Gly<sup>708</sup> also participates in an  $\alpha/\beta$  interaction that regulates activation lends additional credence to this hypothesis and suggests that the TM helix packing interface proposed here is a nexus for bidirectional transmembrane signaling through integrins.

## Reference List

1. Hynes, R. O. (2002) *Cell* **110**, 673-687
2. Campbell, I. D. and Ginsberg, M. H. (2004) *TIBS* **29**, 429-435
3. Hughes, P. E., Diaz-Gonzalez, F., Leong, L., Wu, C., McDonald, J. A., Shattil, S. J., and Ginsberg, M. H. (1996) *J.Biol.Chem.* **271**, 6571-6574
4. Takagi, J., Erickson, H. P., and Springer, T. A. (2001) *Nat.Struct.Biol.* **8**, 412-416
5. Lu, C., Takagi, J., and Springer, T. A. (2001) *J.Biol.Chem.* **276**, 14642-14648
6. Kim, M., Carman, C. V., and Springer, T. A. (2003) *Science* **301**, 1720-1725
7. Luo, B. H., Springer, T. A., and Takagi, J. (2004) *PLoS.Biol.* **2**, 776-786
8. Vinogradova, O., Velyvis, A., Velyviene, A., Hu, B., Haas, T., Plow, E., and Qin, J. (2002) *Cell* **110**, 587
9. Ulmer, T. S., Yaspan, B., Ginsberg, M. H., and Campbell, I. D. (2001) *Biochemistry* **40**, 7498-7508
10. Li, R., Babu, C. R., Lear, J. D., Wand, A. J., Bennett, J. S., and DeGrado, W. F. (2001) *Proc.Natl.Acad.Sci.USA* **98**, 12462-12467
11. Schneider, D. and Engelman, D. M. (2004) *J.Biol.Chem.* **279**, 9840-9846
12. Gottschalk, K. E., Adams, P. D., Brunger, A. T., and Kessler, H. (2002) *Protein Sci.* **11**, 1800-1812
13. Adair, B. D. and Yeager, M. (2002) *Proc.Natl.Acad.Sci U.S.A* **99**, 14059-14064
14. O'Toole, T. E., Mandelman, D., Forsyth, J., Shattil, S. J., Plow, E. F., and Ginsberg, M. H. (1991) *Science* **254**, 845-847
15. Shattil, S. J., Hoxie, J. A., Cunningham, M., and Brass, L. F. (1985) *J.Biol.Chem.* **260**, 11107-11114
16. Frelinger, A. L., III, Du, X., Plow, E. F., and Ginsberg, M. H. (1991) *J.Biol.Chem.* **266**, 17106-17111
17. Kouns, W. C., Kirchhofer, D., Hadvary, P., Edenhofer, A., Weller, T., Pfenninger, G., Baumgartner, H. R., Jennings, L. K., and Steiner, B. (1992) *Blood* **80**, 2539-2547
18. Hermes, J. D., Parekh, S. M., Blacklow, S. C., Koster, H., and Knowles, J. R. (1989) *Gene* **84**, 143-151

19. O'Toole, T. E., Katagiri, Y., Faull, R. J., Peter, K., Tamura, R. N., Quaranta, V., Loftus, J. C., Shattil, S. J., and Ginsberg, M. H. (1994) *J.Cell Biol.* **124**, 1047-1059
20. Hughes, P. E., O'Toole, T. E., Ylanne, J., Shattil, S. J., and Ginsberg, M. H. (1995) *J.Biol.Chem.* **270**, 12411-12417
21. Kim, S., Chamberlain, A. K., and Bowie, J. U. (2003) *J Mol.Biol* **329**, 831-840
22. Armulik, A., Nilsson, I., von Heijne, G., and Johansson, S. (1999) *J.Biol.Chem.* **274**, 37030-37034
23. Stefansson, A., Armulik, A., Nilsson, I., von Heijne, G., and Johansson, S. (2004) *J Biol Chem.* **279**, 21200-21205
24. Bower, M. J., Cohen, F. E., and Dunbrack, R. L., Jr. (1997) *J.Mol.Biol.* **267**, 1268-1282
25. Kelley, L. A., Gardner, S. P., and Sutcliffe, M. J. (1996) *Protein Eng* **9**, 1063-1065
26. Kim, S., Chamberlain, A. K., and Bowie, J. U. (2003) *J.Mol.Biol.* **329**, 831-840
27. Melnyk, R. A., Kim, S., Curran, A. R., Engelman, D. M., Bowie, J. U., and Deber, C. M. (2004) *J.Biol.Chem.* **279**, 16591-16597
28. Kim, S., Chamberlain, A. K., and Bowie, J. U. (2004) *Biophys.J.* **87**, 792-799
29. Kim, S., Chamberlain, A. K., and Bowie, J. U. (2004) *Proc.Natl.Acad.Sci.U.S.A* **101**, 5988-5991
30. Li, R., Mitra, N., Gratkowski, H., Vilaire, G., Litvinov, R., Nagasami, C., Weisel, J. W., Lear, J. D., DeGrado, W. F., and Bennett, J. S. (2003) *Science* **300**, 795-798
31. de Planque, M. R. and Killian, J. A. (2003) *Mol.Membr.Biol.* **20**, 271-284
32. Patil, S., Jedsadayanmata, A., Wencel-Drake, J. D., Wang, W., Knezevic, I., and Lam, S. C. (1999) *J.Biol.Chem.* **274**, 28575-28583
33. Ulmer, T. S., Calderwood, D. A., Ginsberg, M. H., and Campbell, I. D. (2003) *Biochemistry* **42**, 8307-8312
34. Diaz-Gonzalez, F., Forsyth, J., Steiner, B., and Ginsberg, M. H. (1996) *Mol.Biol.Cell* **7**, 1939-1951
35. Guan, J.-L., Trevithick, J. E., and Hynes, R. O. (1991) *CR* **2**, 951-964
36. Miyamoto, S., Akiyama, S. K., and Yamada, K. M. (1995) *Science* **267**, 883-885
37. Xiong, J. P., Stehle, T., Diefenbach, B., Zhang, R., Dunker, R., Scott, D. L., Joachimiak, A., Goodman, S. L., and Arnaout, M. A. (2001) *Science* 1064535

38. Takagi, J., Strokovich, K., Springer, T. A., and Walz, T. (2003) *EMBO J* **22**, 4607-4615
39. Hantgan, R. R., Paumi, C., Rocco, M., and Weisel, J. W. (1999) *Biochemistry* **38**, 14461-14474
40. LaFlamme, S. E., Akiyama, S. K., and Yamada, K. M. (1992) *J. Cell Biol.* **117**, 437-447
41. Hynes, R. O. (2003) *Science* **300**, 755-756

## FIGURE LEGENDS

**Fig. 1. “Windows” for random mutagenic analysis of transmembrane and cytoplasmic domains of the  $\beta 3$  integrin subunit.** The coding region for the  $\beta 3$  transmembrane and cytoplasmic domains was divided into four “windows”. Each window contains 66 nucleotides corresponding to the amino acid sequences with a nine nucleotides overlap between windows.

**Fig. 2. Polymerase chain reactions for construction of random mutagenic cDNA libraries of the  $\beta 3$  transmembrane and cytoplasmic domain.** A. Schematic presentation of the partial  $\beta 3$  cDNA sequence. F.P. and R.P. represent forward primer and reverse primer, respectively, that were derived from the  $\beta 3$  sequence and used in PCR reactions described in B and C. \* represents the stop codon of  $\beta 3$  sequence. Newly created *Sph* I site in the  $\beta 3$  sequence and *Xba* I site present in the vector sequence are indicated. B. Schematic presentation of two consecutive PCR reactions for construction of random mutagenic cDNA library for each “window” of the  $\beta 3$  transmembrane and cytoplasmic domains. The position of each “window” is indicated. C. PCR product (PCR-I in Fig. 3B) for each “window”. PCR-I reaction was performed as described in “Materials and Methods”. 10  $\mu$ l of PCR product from each “window” was separated on 1 % agarose gel and stained with ethidium bromide. The sizes of cDNAs are indicated.

**Fig. 3. Isolation and characterization of clonal cell lines that express activated  $\alpha$ IIb $\beta$ 3 integrin mutants.** A. Pooled stable colonies transfected with each random

mutagenic cDNA library of the  $\beta 3$  transmembrane and cytoplasmic domains were stained with antibodies BD-57 and PAC1 as described in “Materials and Methods”. The cells that revealed both BD-57 and PAC1 staining (gate R2) were single cell-sorted into 96-well plates filled with selection medium. B. FACS analysis of A5 cells and a representative clonal cell line that expresses activating  $\alpha \text{IIb}\beta 3$  integrin mutant.

**Fig. 4. Identified activating mutations in the  $\beta 3$  transmembrane and cytoplasmic domains.** The activating mutations identified in the  $\beta 3$  transmembrane and cytoplasmic domains are listed separately. Number of events for each mutation is indicated in brackets. & represents different mutations identified in the same clone.

**Fig. 5. Frequency of activating mutations in the  $\beta 3$  transmembrane and cytoplasmic domains.** Frequency of activating mutations is plotted against each amino acid residue in the  $\beta 3$  transmembrane and cytoplasmic domains. Amino acid sequence of the  $\beta 3$  transmembrane and cytoplasmic domains is illustrated.

**Fig. 6. Dimer models of integrin  $\alpha \text{IIb}$  and  $\beta 3$  subunits' TMD.** A. Structure A) Calculated model shows a left-handed helix-crossing angle of  $30^\circ$  with crossing point near C-terminus. Packing residues are colored on the dimer model and indicated on the TMD sequence. From the packing residues, G708 mediates the most-close packing. Alternative packing Structure B) Model structure shows a left-handed helix-crossing angle of  $40^\circ$  with crossing point near N-terminus. B. Interhelical residues involved in Structure A.  $\alpha \text{IIb}$  residues are highlighted in green,  $\beta 3$  residues are highlighted in red.

**Fig. 7. Site direct mutagenesis supports simulation Structure A as the inactive state conformation.** A. CHO cells were transfected with plasmid coding for wt and mutant versions of  $\alpha$ I**IIb** and  $\beta$ 3. Shown here a representative dot plots of FACS analysis for cells transfected with wildtype and G708I mutant integrin. Harvested cells were stained for integrin expression (D-57) and activated  $\alpha$ I**IIb $\beta$ 3 (PAC1). B. Activation indices for wildtype and site-directed mutants  $\beta$ 3(I704A),  $\beta$ 3(G708I),  $\alpha$ I**IIb**(T981I) were calculated by measuring PAC1 staining in the presence or absence of Anti-LIBS6 and Ro43-5054 (see Methods). C. Random and site-directed activating mutants map to interhelical residues outlined in computer simulation Structure A (underlined amino acids). Sites of activating random and site-directed mutations are shown with rectangles and circles respectively.**

**Table I. Clonal Cell Lines With Activated  $\alpha\text{II}\beta\text{3}$** 

Window	Cell Lines Isolated	Activation Re-Confirmed	Unique Mutations Identified
I	288	91	7
II	468	192	22
III	65	5	0
IV	30	0	0

## Table II. Activating $\beta$ 3 Transmembrane Mutations

### Mutations that directly shorten the TM helix (Loop-out and truncation mutations)

$\Delta(\text{Val}^{695}\text{Val}^{696})$   
Leu<sup>697</sup>->Pro &  $\Delta(\text{Leu}^{698}\text{Ser}^{699}\text{Val}^{700})$   
 $\Delta(\text{Ser}^{699}\text{Val}^{700})$   
Leu<sup>709</sup>->His &  $\Delta(\text{Leu}^{697}\text{Leu}^{698})$   
Trp<sup>715</sup>->Stop

### Mutations that are predicted to shorten the TM helix (Apolar to charged mutations)

Leu<sup>697</sup>->Arg  
Leu<sup>712</sup>->Arg  
Leu<sup>713</sup>->His  
Trp<sup>715</sup>->Arg

### Mutations that are not predicted to shorten the TM helix

Gly<sup>708</sup>->Ser  
Ala<sup>711</sup>->Thr & Thr<sup>720</sup>->Ala  
Ile<sup>714</sup>->Thr  
Ile<sup>714</sup>->Thr &  $\Delta(\text{Ile}^{721})$

Figure 1

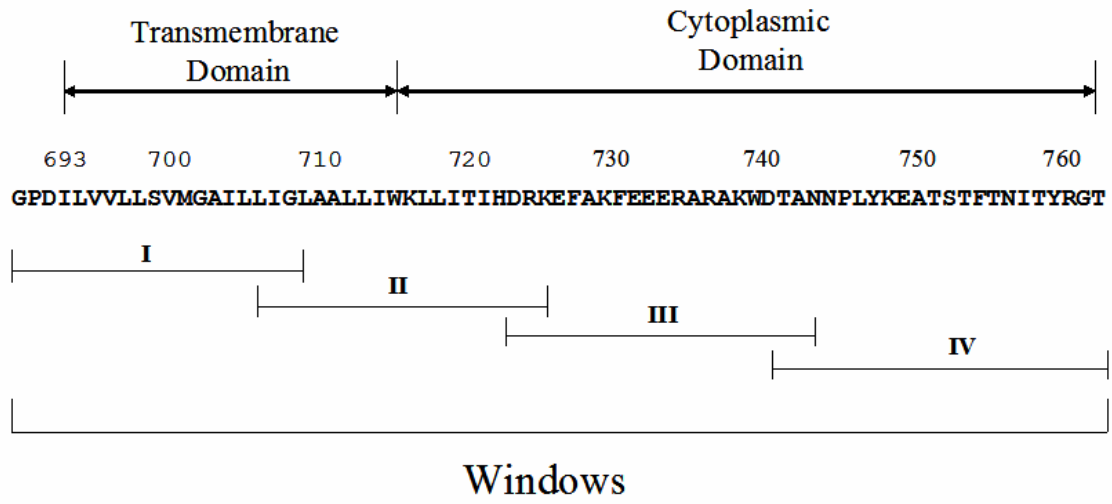


Figure 2A

Partial  $\beta 3$  cDNA

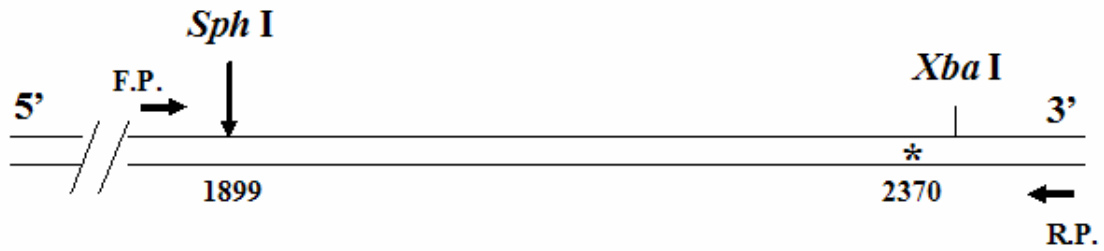


Figure 2B

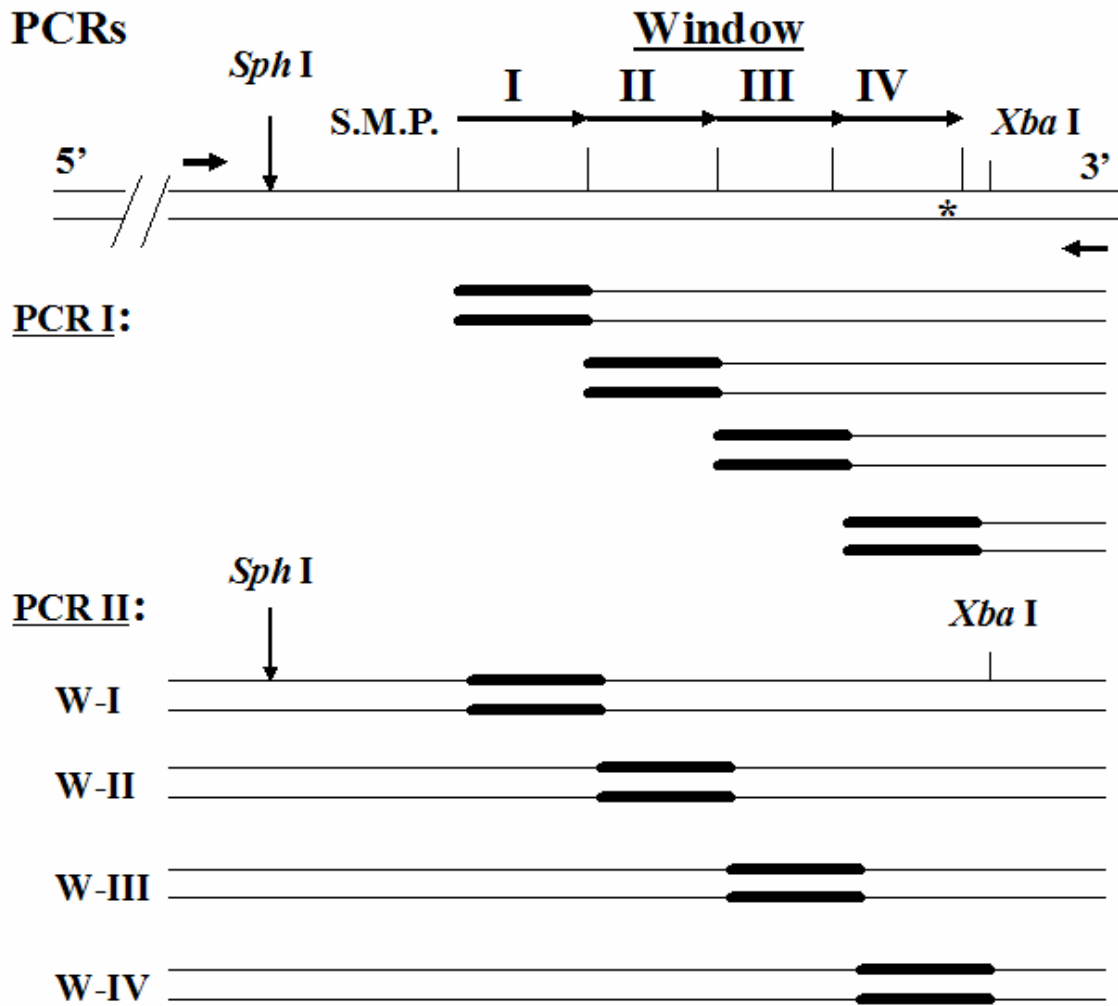


Figure 2C

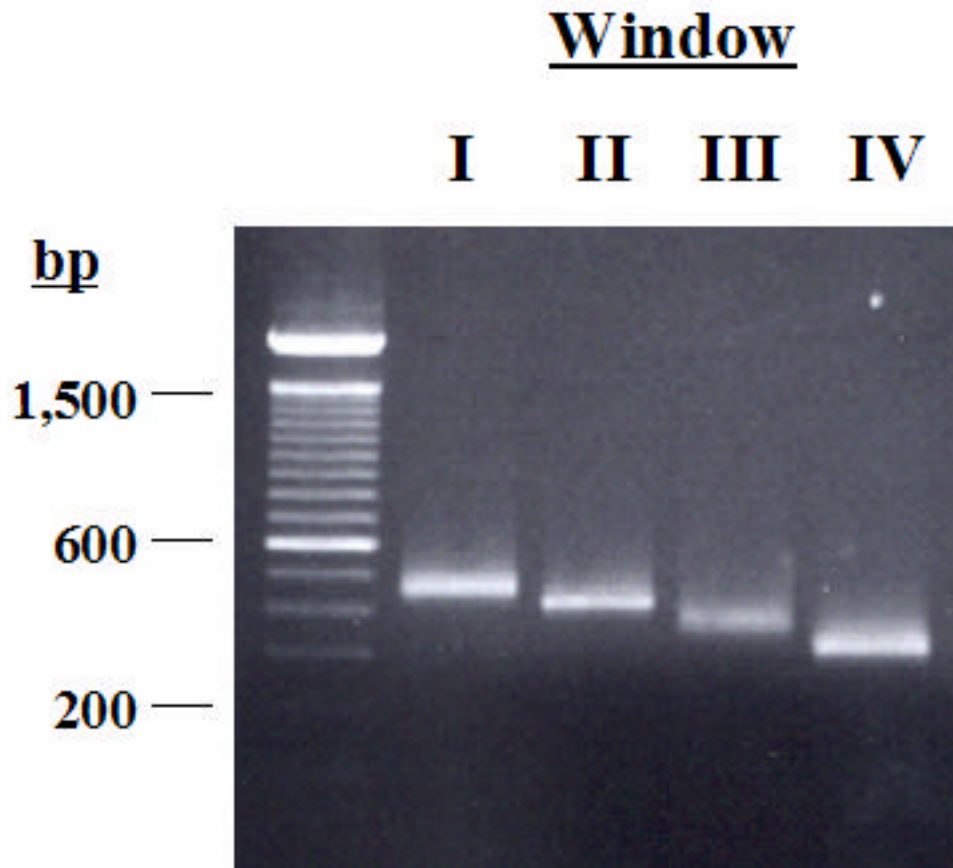
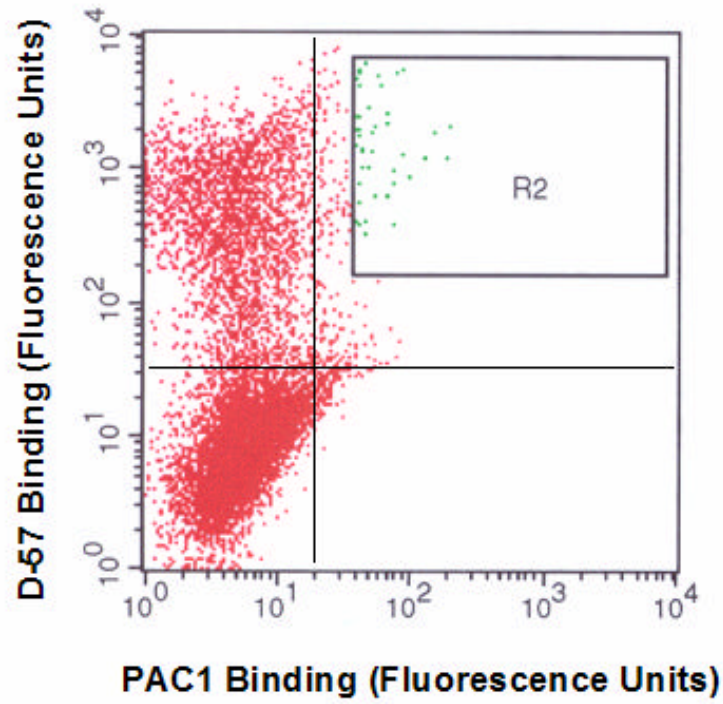


Figure 3

**A.**



**B.**

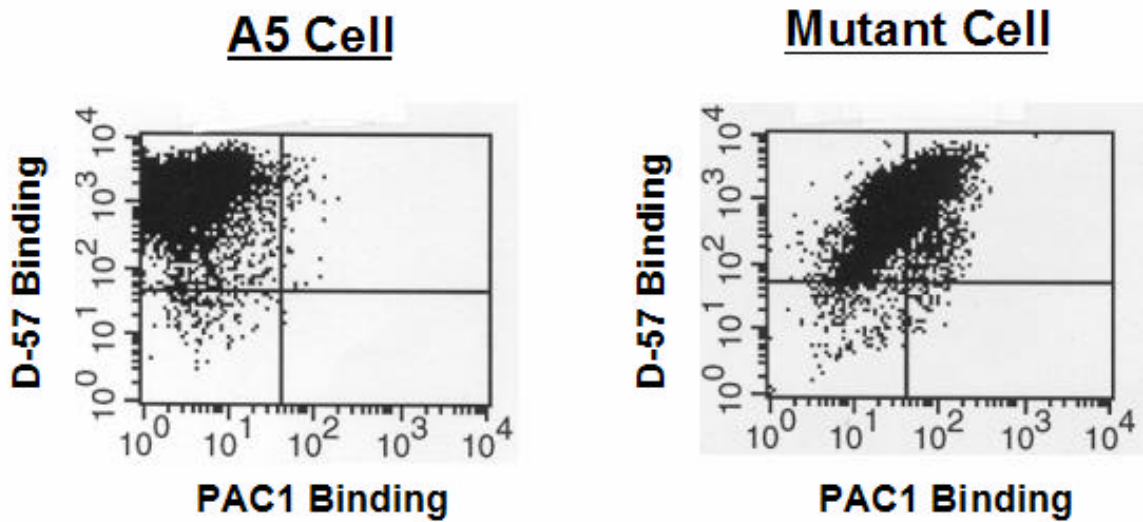


Figure 4

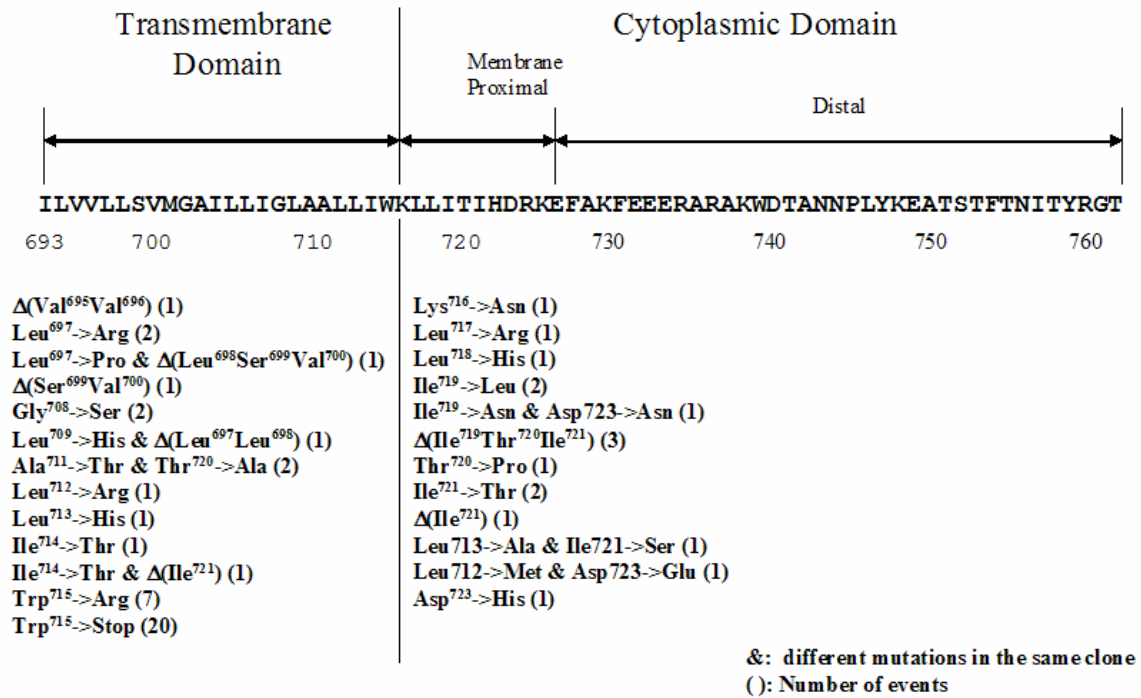


Figure 5

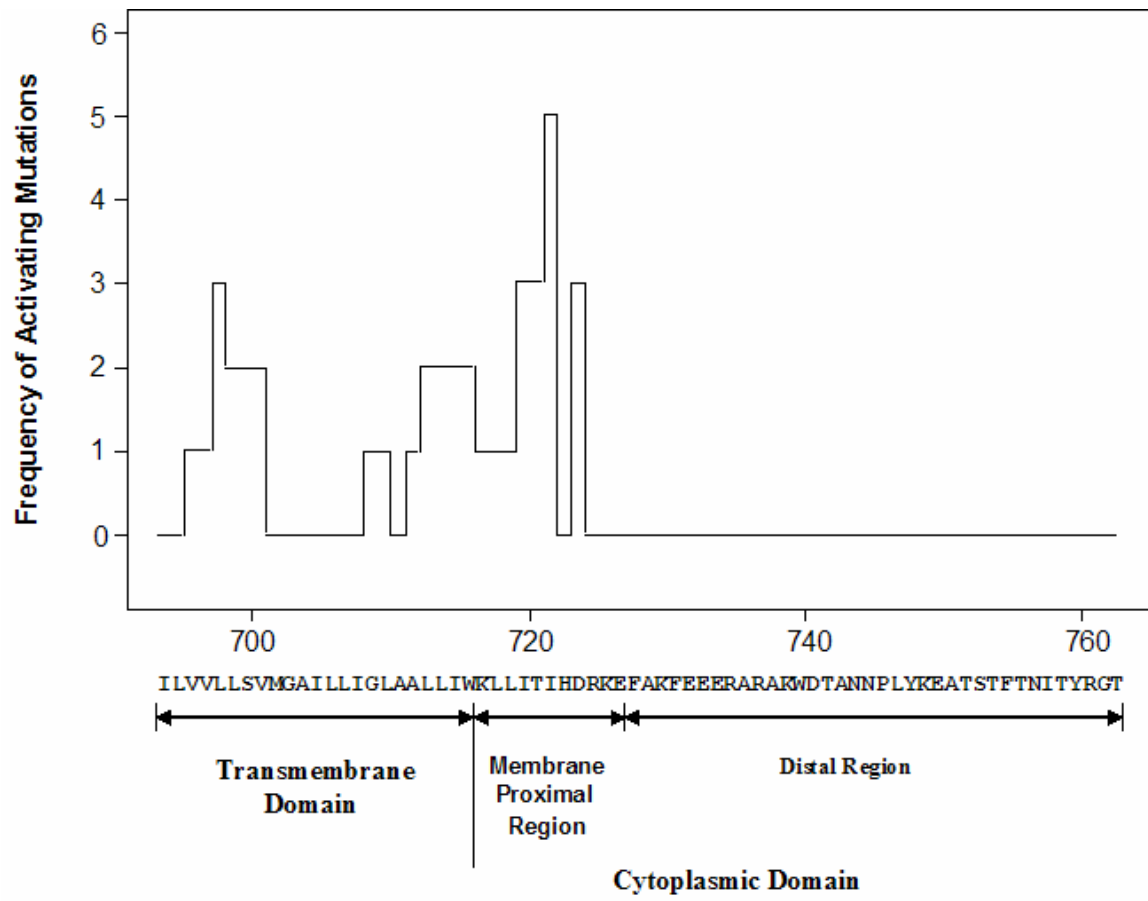




Figure 7A

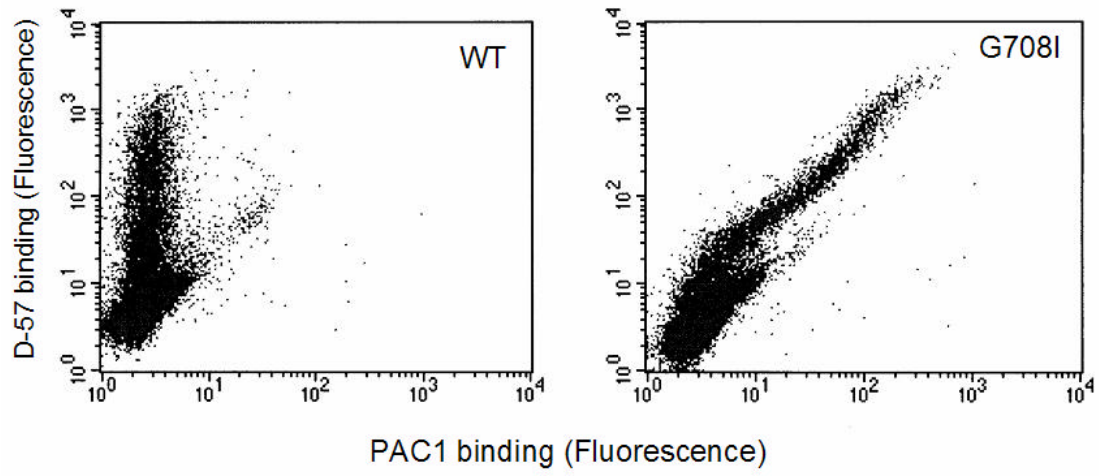


Figure 7B

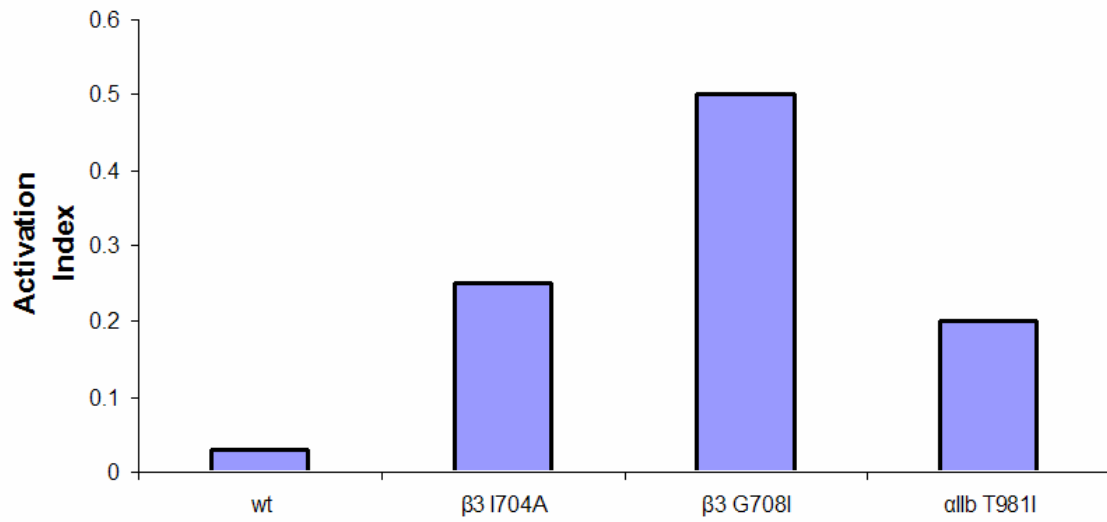


Figure 7C

967 989  
 $\alpha$ I Ib WWVLVGVLGGLLLI<sup>○</sup>ILVLAMWK  
 $\beta$ 3 LVLLSVMGAD<sup>○</sup>LLI<sup>□</sup>GLA<sup>□</sup>ALL<sup>□</sup>WK  
694 716